Conformations and Receptor Activity of Desmopressin Analogues, Which Contain γ-Turn Mimetics or a $\Psi[CH_2O]$ Isostere

Mattias Hedenström,[†] ZhongQing Yuan,[†] Kay Brickmann,[†,‡] Jolanta Carlsson,[§] Kjell Ekholm,[§] Birgitta Johansson,[§] Eva Kreutz,[§] Anders Nilsson,[§] Ingmar Sethson,[†] and Jan Kihlberg*[,†]

Organic Chemistry, Department of Chemistry, Umeå University, SE-901 87 Umeå, Sweden, and Ferring AB, P.O. Box 30047, SE-20061 Limhamn, Sweden

Received October 26, 2001

Three analogues of the antidiuretic drug desmopressin ([1-desamino,8-D-arginine]vasopressin) have been prepared. In two of these, γ-turn mimetics based on a morpholin-3-one framework have been inserted instead of residues Phe3−Asn5, whereas the third analogue has a methylene ether isostere in place of the amide bond between residues 3 and 4. The three analogues were used to probe if the structure determined for desmopressin in aqueous solution, which contains an inverse γ-turn centered around Gln4, is important in interactions with the vasopressin V_2 receptor. Conformational studies revealed that the analogues that contain either an inverse γ-turn mimetic or a methylene ether isostere mimicked the conformation of desmopressin fairly well and very well, respectively. Despite this, the analogues displayed only very low agonistic activities at the vasopressin V_2 receptor. Consequently, an inverse γ-turn involving residues Phe3−Asn5 does not appear to be important when desmopressin is bound to the V_2 receptor. In addition, it was concluded that the amide bond between Phe3 and Gln4 in desmopressin is crucial for interactions with the antidiuretic V_2 receptor.

Introduction

The neurohypophyseal peptide hormone vasopressin[1] (**1**, Figure 1) interacts with several members of the G-protein-coupled receptor family.[2] Activity at the V_2 receptor is responsible for the antidiuretic properties of vasopressin, whereas interactions with the V_{1a} and V_{1b} receptors control blood pressure, as well as some other properties. Deamination of Cys1 and simultaneous replacment of L-Arg8 with D-Arg in **1** yields the potent antidiuretic drug desmopressin **2**.[3,4] Desmopressin does not cause vasoconstriction and contraction of smooth muscles in the uterus or in the intestines as the original peptide hormone does and is used in treatment of diabetes insipidus, haemophilia A, von Willebrand's disease, and thrombocyte dysfunction prior to surgery.[3,5,6]

The use of peptides as drugs is often limited by their poor pharmacokinetic properties, namely, low uptake on oral administration, rapid enzymatic degradation, and facile excretion.[7] In addition, flexibility of the peptide may reduce the biological activity and the receptor selectivity. To circumvent these problems, large efforts have been made to design and synthesize peptidomemetics, which have different structures than the parent peptides but nevertheless act as ligands to the same receptor.[8−12] Several requirements should be fulfilled by peptidomimetics. The topographical relationship between the functional groups of the mimetic should resemble those of the peptide, and it is essential that functionalities corresponding to side chains can be introduced at desired positions with correct spatial arrangement. It is also an advantage if the synthetic route is short and efficient.

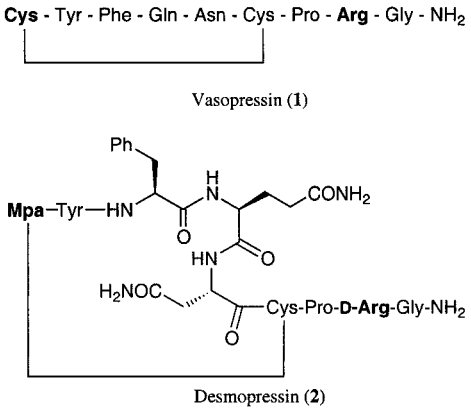

Figure 1. Structures of the peptide hormone vasopressin and the drug desmopressin. Differences are indicated in bold.

The conformation of desmopressin when bound to a G-protein-coupled receptor is not known, but the structure of desmopressin alone has been studied by two-dimensional nuclear magnetic resonance (NMR) spectroscopy in aqueous solution with or without addition of trifluoroethanol.[13,14] In addition, the structure of desmopressin when bound to the carrier protein neurophysin has been determined by NMR spectroscopy.[15] A large number of similar conformational studies have also been performed for vasopressin and several of its other analogues.[16−21] In general, all of these studies reveal that the macrocyclic ring of desmopressin and vasopressin adopts β- or γ-turn structures, with a highly flexible acyclic tail.

In aqueous solution, and at a pH close to physiological conditions, desmopressin (**2**) was found to contain a

* To whom correspondence should be addressed. Tel.: +46-90-786 68 90. Fax: +46-90-13 88 85. E-mail: jan.kihlberg@chem.umu.se.
† Umeå University.
‡ Present address: Medicinal Chemistry, AstraZeneca R&D Mölndal, SE-431 83 Mölndal, Sweden.
§ Ferring AB.

10.1021/jm011073b CCC: $22.00
Published on Web 05/04/2002

Scheme 1. Three Analogues of Desmopressin (**4**, **6**, and **8**) Prepared by Solid Phase Synthesis

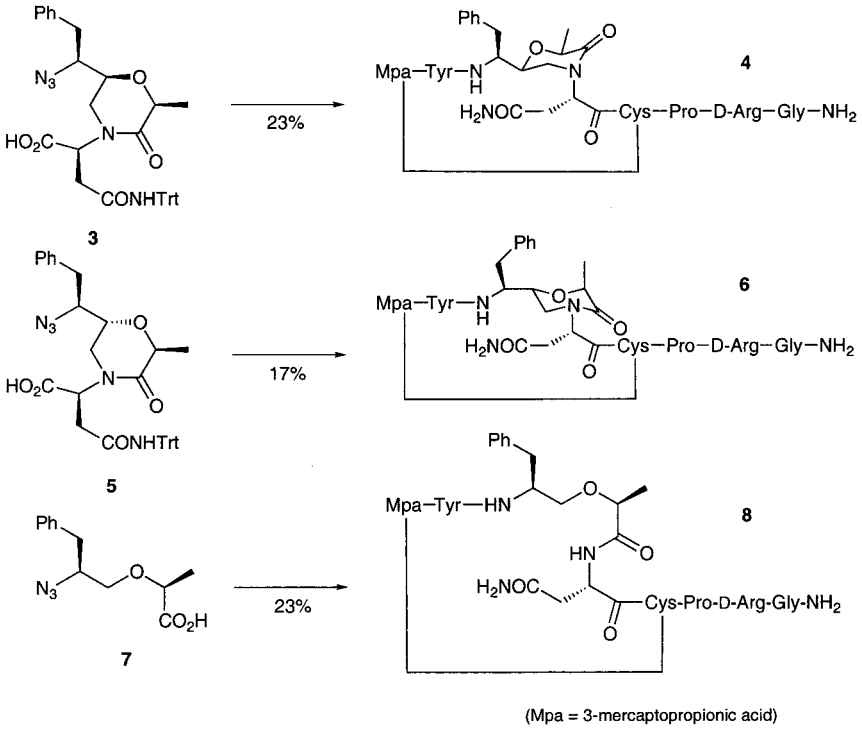

stable inverse γ-turn centered around Gln4.[14] Interestingly, such a γ-turn was also predicted when vasopressin was docked into a three-dimensional computer model of the V_{1a} receptor.[22] Formation of a hydrogen bond between the CO of Phe3 and the NH of Asn5, which generates a γ-turn (Figure 1), is thus conformationally favorable in desmopressin and may be compatible with receptor binding. To probe if a Phe3−Asn5 γ-turn in desmopressin is important in interactions with the V_2 receptor, we have prepared three analogues of desmopressin, two of which contain mimetics of γ-turns in place of residues Phe3−Asn5. The antidiuretic activities of the analogues were determined, and their solution structures were investigated by ^{1}H NMR spectroscopy.

Results and Discussion

Design and Synthesis. Analogues **4**, **6**, and **8** (Scheme 1) were designed to investigate if the inverse γ-turn found for residues Phe3−Asn5 in aqueous solutions of desmopressin is essential also in interactions with G-protein-coupled receptors. To simplify the synthesis of these analogues, Gln at position 4 of desmopressin was replaced by Ala. This replacement still allows structure−activity comparisons of desmopressin with the three analogues since a Gln4→Ala substitution in desmopressin has only a minor effect on the activity at the kidney V_2 receptor (cf. Table 1).[23,24] In addition, it is most unlikely that the secondary structure of desmopressin is influenced by a Gln4→Ala substitution since Gln4 can be replaced by such a structurally different residue as a glycosylated serine without affecting the conformation.[25]

In analogues **4** and **6**, the amide bond between residues i and $i + 1$ of the turn in **2** has been exchanged for a $\Psi[CH_2O]$ isostere, simultaneously with replacement of the hydrogen bond between residues i and $i + 2$ with a methylene bridge. Consequently, the seven-membered, hydrogen-bonded γ-turn in **2** has been replaced by a six-membered morpholin-3-one ring.[26] This reduces the flexibility of the peptide backbone and should prevent enzymatic degradation after Phe3, a position which is otherwise susceptible to cleavage by chymotrypsin.[27] Ab initio calculations have shown that morpholin-3-ones constitute excellent mimetics of either inverse or classical γ-turns, depending on the choice of stereochemistry at C-6 of the morpholinone ring.[26] In **4**, the $i + 1$ side chain is located in a pseudoequatorial position, as in the inverse γ-turn found in desmopressin in aqueous solution, whereas the $i + 1$ side chain in **6** is in a pseudoaxial orientation, just as in a classical γ-turn. In desmopressin analogue **8**, the amide bond between residues 3 and 4 is instead replaced by a methylene ether isostere. Just as for **4** and **6**, this prevents enzymatic cleavage after Phe3, but the lack of conformational restraints should allow **8** to adopt other conformations than mimetics **4** and **6**.

γ-Turn mimetics **3** and **5** were prepared as described earlier.[26] Synthesis of the methylene ether isostere **7** started from commercially available (2*S*)-phenylalaninol (**9**, Scheme 2). Initial attempts to prepare analogues of **7**, in which the amino group was protected with either

Table 1. In Vivo Antidiuretic Activity of Vasopressin and Analogues

peptide	n[a]	agonist activity[b] (IU/mg)
vasopressin (**1**)		561
desmopressin (**2**)		1000
[Ala^4]desmopressin		645
4	5	$<2 \times 10^{-3}$
6	6	2.6×10^{-3} ($\pm 3.7 \times 10^{-4}$)
8	7	0.56 ($\pm 7.2 \times 10^{-2}$)

[a] Number of experiments. [b] The antidiuretic activity was calculated using a vasopressin house standard (561 IU/mg) calibrated against an international vasopressin standard. Values are mean (±SEM).

Scheme 2[a]

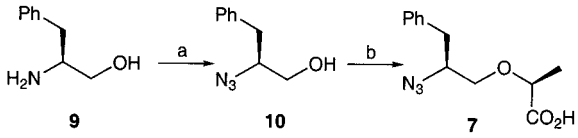

[a] Reagents: (a) TfN_3, DMAP, $CuSO_4$, CH_2Cl_2, room temperature, 2 h; 68%. (b) *R*-(−)-2-Chloropropionic acid, NaH (50% oil suspension), 1,4-dioxane, room temperature, 20 h; 48%.

a *tert*-butoxycarbonyl (Boc) or a 9-fluorenylmethoxycarbonyl (Fmoc) group, by different routes were hampered by low overall yields and formation of impure products.[28] Because azides can be conveniently reduced to amines on solid phase, the azido group was instead chosen as a protective group for **7**.[26,29] Conversion of **9** to azido alcohol **10** was achieved in a copper-catalyzed diazo transfer reaction using freshly prepared triflic azide.[30,31] Base-promoted *O*-alkylation of **10** to give **7** was carried out with both (2*R*)-2-chloro- and (2*R*)-2-bromopropionic acid to establish if the choice of leaving group influenced the amount of epimerization of the propionic acid moiety.[32] In this case, use of 2-chloropropionic acid together with sodium hydride as base gave **7** in 48% yield and excellent diastereoselectivity (97:3) according to ^{1}H NMR spectroscopy. When 2-bromopropionic acid was used under identical conditions, **7** was obtained in 68% yield but as a 4:1 diastereomeric mixture, which was most difficult to separate.

Compounds **3**, **5**, and **7** were then used as building blocks to prepare **4**, **6**, and **8**, respectively, using solid phase synthesis (Scheme 1). This was performed on a polystyrene resin grafted with poly(ethylene glycol) chains (TentaGel S NH_2) functionalized with the Rink amide linker.[33,34] N^{α}-Fmoc amino acids carrying standard side chain protective groups were coupled to the resin as benzotriazolyl (HOBt) esters,[35] whereas mimetics **3**, **5**, and **7** were activated as the more reactive 7-azabenzotriazolyl (HOAt) esters.[36] When the mimetics had been attached to the solid phase, the azido group was reduced by treatment with tin(II) chloride in the presence of thiophenol and triethylamine.[29] The progress of the reduction was conveniently monitored by the disappearance of the N_3 stretch in the IR spectrum obtained from a few resin beads.[37] After cleavage from the solid phase and side chain deprotection by treatment with trifluoroacetic acid, disulfide bond formation was affected by oxidation with iodine in methanol.[25] Finally, purification by reversed-phase high-performance liquid chromatography (HPLC) gave desmopressin analogues **4**,[26] **6**, and **8**, each in ∼20% overall yield. The structures of the three desmopressin analogues were confirmed by mass and NMR spectroscopy (cf. Tables 2, 3, and 5).

Pharmacological Studies. The antidiuretic effect of desmopressin analogues **4**, **6**, and **8** at the V_2 receptor was determined after intravenous administration to anaesthetized rats (Table 1). Analogues **4** and **6**, which contain γ-turn mimetics, were both more than 5 orders of magnitude less active than vasopressin and desmopressin. The methylene ether isostere **8**, which lacks the conformational restriction imposed by the γ-turn mi-

Table 2. Temperature Coefficients (Δδ/ΔT, ppb/K) and ^{1}H and ^{13}C NMR Chemical Shifts (δ, ppm) for Peptide **4** in Aqueous Solution[a]

residue	Δδ/ΔT[b]	NH	CαH	CβH	CγH	other
Mpr1			2.61[c]	2.82, 3.30		
			35.6	36.2		
Tyr2	−6.7	8.32	4.13	2.41[c]		6.72(Hδ), 6.66(Hε)
			59.1	37.9		131.0(Cδ), 117.1(Cε)
Phe3	−6.7	7.73	4.26	2.88, 2.95		7.26(Hδ), 7.31(Hε), 7.20(Hζ)
			52.7	38.2		131.3(Cδ), 130.5(Cε), 128.7(Cζ)
methylene bridge						3.91(H1), 3.69(H2), 3.26(H2′), 76.0(C1), 52.4(C2)
Ala4			4.28	1.43[c]		
			76.3	18.2		
Asn5			4.27	2.65, 2.90		6.91 and 7.72($N\delta H_2$)
			61.1	39.8		
Cys6	−7.8	8.12	4.64	2.86, 3.13		
			57.1	37.9		
Pro7			4.37	1.83, 2.24	1.99[c]	3.56 and 3.83(Hδ)
			62.5	31.0	26.4	49.7(Cδ)
D-Arg8	−11.0	8.89	4.19	1.70, 1.85	1.58[c]	3.12[c](Hδ), 7.23(NεH)
			55.7	29.1	26.2	42.1(Cδ)
Gly9	−4.7	8.33	3.81, 3.86			7.18 and 7.32($CONH_2$)
			43.4			

[a] Obtained at 600 MHz in water containing 10% D_2O at 278 K and pH 6.7 with H_2O (δ_H 4.98 ppm) as internal standard. [b] The amide proton coefficients were all linear with $R^2 > 0.99$. [c] Degeneracy has been assumed.

Table 3. ^{1}H NMR Chemical Shifts (δ, ppm) for Peptide **6** in Aqueous Solution[a]

residue	NH	CαH	CβH	CγH	other
Mpr1		2.92[b]	2.47, 2.55		
Tyr2	8.22	4.17	2.47, 2.51		6.74(Hδ), 6.65(Hε)
Phe3	7.67	4.47	2.68, 2.98		7.28(Hδ), 7.35(Hε), 7.25(Hζ)
Ala4		4.40	1.34[b]		
methylene bridge					4.19(H1), 3.40(H2), 3.46(H2′)
Asn5		5.36	2.75, 2.92		6.99 and 7.74($N\delta H_2$)
Cys6	8.69	5.03	2.76, 3.27		
Pro7		4.41	1.88, 2.27	2.00[b]	3.64, 3.75(Hδ)
D-Arg8	8.90	4.26	1.71, 1.87	1.60[b]	3.16[b](Hδ), 7.28(NεH)
Gly9	8.46	3.85[b]			7.20 and 7.42($CONH_2$)

[a] Obtained at 600 MHz in water containing 10% D_2O at 278 K and pH 6.7 with H_2O (δ_H 4.98 ppm) as internal standard. [b] Degeneracy has been assumed.

Table 4. Hydrogen Bonds and Their Relative Frequency in the Accepted Structures of Peptide **4**

donor	acceptor	angle[a] (deg)	dist.[b] (Å)	A[c] (%)	B[c] (%)
D-Arg8 **H**N	Cys6 **O**	135	1.8	100	100
Gly9 **H**N	Cys6 **O**	154	2.5	13	29

[a] The donor−hydrogen−acceptor angle criterion was 120−180°. [b] The hydrogen−acceptor distance criterion was ≤3.0 Å. [c] Structure families A and B, respectively.

metics, had a substantially higher antidiuretic effect than **4** and **6** but was still 3 orders of magnitude less potent than **1** and **2**. However, a dose−response curve was obtained for both analogues **6** and **8**, for doses below 0.2 mg/rat, revealing that they were able to bind to the receptor and elicit a message. It was also found that the three analogues did not show any activity as vasopressin receptor antagonists when evaluated in vivo in rats. The low activity at the V_2 receptor displayed by **4**, **6**, and **8** can be due to the structural modifications of the analogues as compared to desmopressin or to an influence from these modifications on the conformational features of the analogues. To differentiate between these possibilities, it was decided to investigate the conformation(s) of analogues **4** and **8** by using ^{1}H NMR spectroscopy. Because an inverse γ-turn was found for desmopressin in aqueous solution, analogue **4**, which contains a mimetic of an inverse γ-turn, was selected for the NMR study instead of **6**, which contains a mimetic of a classical γ-turn.

Structure Determination of Analogue 4. The ^{1}H resonances of desmopressin analogue **4** were assigned by using the conventional strategy[38] from a set of COSY, TOCSY, NOESY, and ROESY spectra obtained in aqueous solutions at 5 °C and pH 6.7 (Table 2).[39] The proton resonances were then used in combination with gradient-enhanced ^{13}C-HSQC spectra to identify the ^{13}C resonances. Large deviations from random coil chemical shifts of backbone NH and Hα in the macrocyclic ring (residues 1−6), even for those residues not involved in the γ-turn mimetic inserted at positions 3−5, indicated a well-ordered structure in this part of **4**. This observation was further supported by the presence of several medium range nuclear Overhauser effects (NOEs). On the other hand, the chemical shifts of the three residue acyclic tail had only small deviations from random coil values, which is an indication of considerable flexibility. A total of 74 distance restraints were derived from the NOESY spectrum. These restraints consisted of 33 intraresidual, 29 sequential, 11 medium, and 1 long-range connectivity. When determining distance restraints, C6 and C5 in the morpholinone ring of the γ-turn mimetic were considered as part of Phe3, and the NOE between Mpr1 Hα and Cys6 NH was regarded as a long-range connectivity. All $^3J_{NH\alpha}$ coupling constants, except that of Phe3, are consistent with conformational averaging and were therefore not utilized in the structure calculations.[40] For Phe3, $^3J_{NH\alpha}$ was found to be 9.6 Hz, which was converted to a ϕ dihedral angle of $-109 \pm 30°$. Because of spectral overlap and degenerated chemical shifts of the β-protons, $^3J_{\alpha\beta}$ could only be determined for Phe3, Cys6, and D-Arg8. Both Phe3 and Cys6, but not D-Arg8, had a $^3J_{\alpha\beta}$ that indicated population of one preferred rotamer about the Cα−Cβ bond, and the χ^1 torsion angles for these two residues were determined to be -50 ± 30 and $-70 \pm 30°$, respectively. Because all amide proton temperature coefficients were more negative than −4.7 ppb/K, no indications of intramolecular hydrogen bonds or steric shielding of protons from solvent that could be used as restraints were found for **4**.

The 74 NOE-derived distance restraints and the three dihedral angle restraints mentioned above were used to determine starting structures for **4** with the program X-PLOR.[41] These structures were then subjected to simulated annealing using an ab initio protocol followed by simulated annealing refinement.[42,43] Somewhat surprisingly, none of the resulting refined structures fulfilled the acceptance criterion of no NOE distance violations >0.3 Å. Such a result could be explained if **4** is flexible so that it can assume two or more conformations that are in fast exchange on the NMR time scale. This would result in time-averaged NOEs that, due to the r^{-6} dependence of the NOE intensities, will overemphasize the restraints that represent short distances.[44] As a consequence, incompatibilities in the

Table 5. Temperature Coefficients (Δδ/ΔT, ppb/K) and ^{1}H and ^{13}C NMR Chemical Shifts (δ, ppm) for Peptide **8** in Aqueous Solution[a]

residue	Δδ/ΔT[b]	NH	CαH	CβH	CγH	other
Mpr1			2.57	2.86, 3.15		
			36.1	35.4		
Tyr2	−7.3	8.35	4.23	2.59, 2.64		6.74(Hδ), 6.68(Hϵ)
			58.4	37.4		132.1(Cδ), 117.2(Cϵ)
Phey[CH_2O]	−1.5	7.19	4.22	2.60, 3.29		7.27(Hδ), 7.37(Hϵ), 7.29(Hζ)
						3.29 and 3.42(CH_2O)
			52.0	38.6		131.3(Cδ), 130.7(Cϵ), 128.8(Cζ)
						72.9(CH_2O)
Ala4			3.95	1.33[c]		
			79.2	20.3		
Asn5	−5.6	8.38	4.82	2.70, 2.75		6.96 and 7.74(NδH_2)
			51.4	37.7		
Cys6	−6.2	8.65	5.02	2.68, 3.18		
			52.3	40.1		
Pro7			4.44	1.9, 2.28	2.01[c]	3.67 and 3.79(Hδ)
			62.6	31.3	27.6	49.8(Cδ)
D-Arg8	−9.1	8.91	4.26	1.73, 1.89	1.60[c]	3.16[c](Hδ)
			55.7	29.5	26.2	42.3(Cδ)
Gly9	−5.3	8.48	3.86[c]			7.20 and 7.43($CONH_2$)
			44.1			

[a] Obtained at 600 MHz in water containing 10% D_2O at 278 K and pH 6.7 with H_2O (δ_H 4.98 ppm) as internal standard. [b] The amide proton coefficients were all linear with $R^2 > 0.99$. [c] Degeneracy has been assumed.

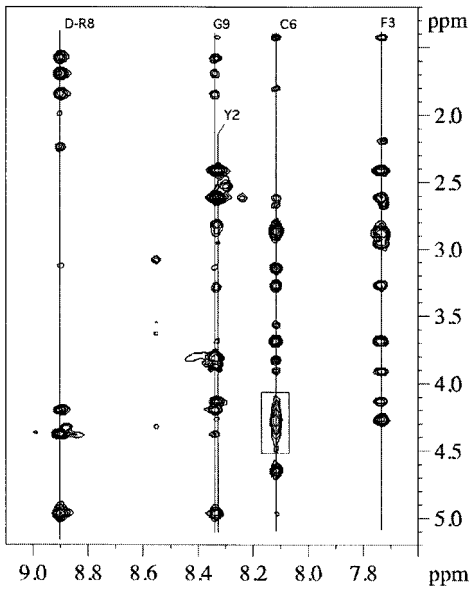

Figure 2. Amide region of the NOESY spectrum of peptide **4** in H_2O/D_2O (9:1) at 278 K and pH 6.7. The boxed cross-peak is between Cys6 NH and Asn5 Hα. The line broadening of Asn5 Hα is easily distinguished.

NOE-derived distance restraints may occur if they represent short distances from different conformations. A closer inspection of the structures calculated for **4** revealed that they could be divided into two families with complementary NOE violations. That is, the distance restraint violations found in one structure family were not found in the other and vice versa. Subsequently, it was possible to derive two sets of distance restraints, each of which was used to calculate two structure families, A and B, that did not show any NOE violations. It appears likely that this conformational exchange process accounts for the large difference in the temperature coefficient of Phe3 NH in **4** (−6.7 ppb/K) as compared to in desmopressin (−2.7 ppb/K). For desmopressin, shielding from the surrounding aqueous solution was proposed to explain the small value of the temperature coefficient of Phe3 NH.[14] In mimetic **4**, this shielding appears to be decreased due to the conformational exchange process between families A and B. Further experimental support for the presence of such a conformational exchange is provided by the observation that the resonance of Asn5 Hα is very broad at low temperature (Figure 2) and becomes substantially narrower when the temperature is raised. The fact that only Asn5 Hα displays significant line broadening, although many other atoms also experience different environments in the two structure families, is due to the large chemical shift difference for Asn5 Hα, as revealed by Gaussian98 calculations[45] for structure families A and B. Accordingly, the exchange process is close to coalescence for Asn5 Hα but in the fast exchange region for the other protons, which experience smaller shift differences upon exchange. However, the observed broadening of the Asn5 Hα resonance implies that the mean lifetime of each conformer is in the millisecond time range. Unfortunately, this relatively slow exchange rate prevented simulations of the exchange process by time-averaged NOE simulations or unrestrained molecular dynamics (MD) calculations, since it would have required prohibitively long simulations to sample the transitions between the conformations.

The structures belonging to each of families A and B differ substantially from each other, especially for the residues found in the macrocyclic ring of **4** (Figure 3). In structure family A, the side chain of Asn5 points toward the center of the macrocyclic ring and the morpholinone ring in the turn mimetic is located in the same plane as the macroyclic ring. In family B, Asn5 points away from the macrocyclic ring whereas the morpholinone ring is perpendicular to the plane of the macrocycle. As a consequence, the backbone of residues 1−6 for the structures in family B assumes a saddlelike fold, which provides a completely different location for the side chain of Ala4 than in family A. In both structure families, the side chains of residues Tyr2 and Phe3 adopt similar orientations with respect to the macrocyclic ring and the morpholinone ring retains its half-chair conformation,[26] with the C-2 methyl group that constitutes the side chain of Ala4 in a pseudoequatorial orientation. The average backbone rmsd from the mean structure of residues 1−6 in the accepted structures of **4** is 0.34 and 0.21 Å for families A and B, respectively, indicating a well-ordered structure for each family, although a certain flexibility can be seen for the disulfide bridge. The rmsd of all heavy atoms in the macrocyclic ring is 0.71 and 0.63 Å for families A and B, respectively. A hydrogen bond between D-Arg8 NH and Cys6 O appears in both structure families (Table 4) and

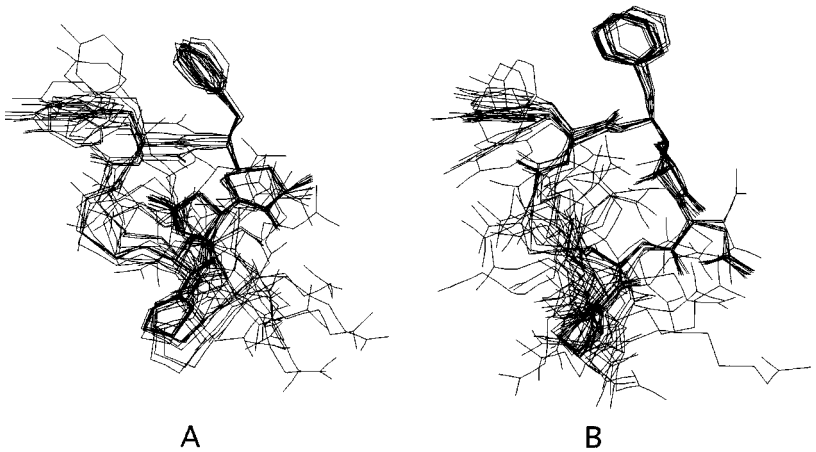

Figure 3. Superimposition of 20 structures, randomly chosen from those calculated for families A (left) and B (right) of peptide **4**.

Figure 4. Superimposition of 20 structures, randomly chosen from those calculated for peptide **8**.

a γ-turn is thus formed over residues 6−8.[46] In some of the accepted structures, a hydrogen bond is also found between Gly9 NH and Cys6 O. This hydrogen bond pattern describes a three residue tail that is quite well-defined for the first residue, Pro7, but which then becomes increasingly more flexible toward the C-terminal Gly9. The similar structure and flexibility of the tail in both structure families indicate that the tail does not participate in the conformational exchange involving the macrocyclic ring. One might speculate that the energy barrier between the two structure families is low since the hydrogen bonds in the tail do not have to be broken to allow the observed conformational exchange.

Structure Determination of Analogue 8. The ^{1}H and ^{13}C resonances of **8** were assigned in the same manner as for desmopressin analogue **4** (Table 5). As in the case of **4**, large deviations from random coil chemical shifts were observed for the residues in the macrocyclic ring, whereas only minor deviations were seen for the three residue tail. Because of some unfortunate spectral overlap, only 55 distance restraints (32 intraresidue, 20 sequential, 2 medium, and 1 long-range) derived from the ROESY spectrum could be used in the structure calculations using a simulated annealing protocol. All of the measured $^3J_{NH\alpha}$ coupling constants were within 5.5−6.7 Hz and thus in the region corresponding to conformational averaging, whereas spectral overlap prevented determination of any $^3J_{\alpha\beta}$ coupling constants. Hence, no ϕ dihedral angle restraints were used in the structure calculations. The small value of the temperature coefficient for Phe3 NH in **8** ($\Delta\delta/\Delta T$ −1.5 ppb/K, Table 5) coincides well with that found for desmopressin (−2.7 ppb/K).[14] Because this small $\Delta\delta/\Delta T$ value for desmopressin is most likely due to shielding from the solvent rather than hydrogen bonding, the Phe3 NH temperature coefficient was not used as a restraint in the structure calculations for **8**. The similarity in the environment for Phe3 NH in **8** and desmopressin was confirmed by the structure calculations described below. After refinement, the structural calculations for **8** resulted in 88 accepted structures out of the 100 that were calculated initially.

In contrast to **4**, no indications of a conformational exchange process were found for **8**; instead, the backbone of residues 1−6 adopts one well-defined conformation (Figure 4). This closely resembles the structures belonging to family A of **4** and has the side chains of residues Tyr2, Phe3, and Ala4 directed away from the macrocyclic ring, whereas Asn5 points toward the center of the macrocycle. The average backbone rmsd from the mean structure of residues 1−6 in **8** was 0.29 Å, whereas the rmsd of the heavy atoms of these residues was 0.56 Å; both values indicated a well-ordered structure. As expected, the three residue tail is quite flexible but some conclusions can be made with regard to its structural preferences. The same hydrogen bonds were found in **8** as in **4**, i.e., between D-Arg8 NH and Cys6 O and between Gly9 NH and Cys6 O (Table 6). The latter hydrogen bond is, however, more frequent, suggesting that the tail has some preference for adopting a β-turn. In addition, a hydrogen bond was found between Cys6 NH and Ala4 O in almost all accepted structures, a fact that can explain the large difference in chemical shift of Cys6 NH as compared to **4**.

Table 6. Hydrogen Bonds and Their Relative Frequency in the Accepted Structures of Peptide **8**

donor	acceptor	angle[a] (deg)	dist.[b] (Å)	relative frequency (%)
Cys6 **H**N	Ala4 **O**	135	2.0	91
D-Arg8 **H**N	Cys6 **O**	134	2.0	36
Gly9 **H**N	Cys6 **O**	148	2.6	50
Gly9 **H**N	Pro7 **O**	138	2.3	9

[a] The donor−hydrogen−acceptor angle criterion was 120−180°. [b] The hydrogen−acceptor distance criterion was ≤3.0 Å.

Comparison of Structure and Activity for Analogues 4 and 8 with Desmopressin. Previously, the structure of **2** has been determined by 2D NMR spectroscopy both in aqueous solution[14] and in aqueous trifluoroethanol.[13,47] In aqueous solution, an inverse γ-turn centered around Gln4 and stabilized by a hydrogen bond between Phe3 CO and Asn5 NH was found. In aqueous trifluoroethanol, a β-turn was observed with Gln4 and Asn5 in the $i + 1$ and $i + 2$ positions. NMR studies of a complex between desmopressin and the carrier protein neurophysin II, which may serve as a model for interactions between **2** and protein receptors, revealed the same β-turn at Gln4 and Asn5 as found in aqueous trifluoroethanol.[15] In this complex, the three residue tail of **2** provides important contacts with neurophysin II and an additional β-turn is found for residues Cys6−Gly9. Modeling of the complex between vasopressin (**1**) and the rat V_{1a} recpetor, based on data from site-directed mutagenesis, suggested that **1** was bound in a cleft between the transmembrane helices so that residues Phe3−Asn5 formed a γ-turn,[22] in a similar way as found for **2** in aqueous solution. It should be stressed that structural studies of desmopressin in solution, when bound by neurophysin II or when modeled in complex with a G-protein-coupled receptor, might not reflect binding of desmopressin to the antidiuretic V_2 receptor. Despite this, these structural studies reveal that **2** has a preference to adopt either γ- or β-turn structures for residues in the macrocylic ring and that the conformation is influenced by the surrounding environment.

Superimposition of the lowest energy structure determined in aqueous solution for **2**, with the minimum energy structures in each of families A and B of analogue **4**, revealed that the inverse γ-turn mimetic had some influence on the conformation of **4** (Figure 5). The rmsd for the backbone atoms of residues 1−6 in the superimposition was 1.31 and 1.80 Å for families A

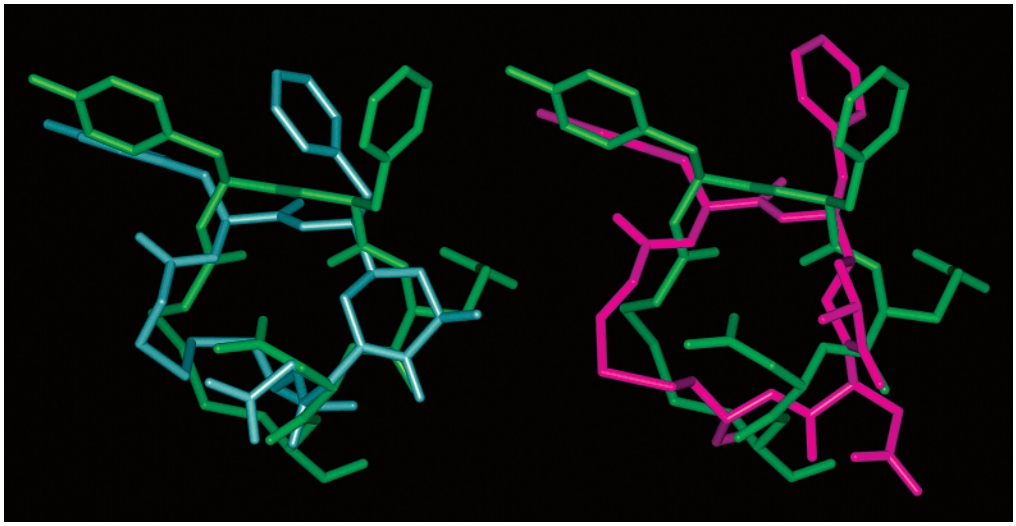

Figure 5. Comparison of the lowest energy structure found in aqueous solution for desmopressin[14] with the lowest energy structures from families A (left) and B (right) of **4**. Desmopressin is represented in green, and the lowest energy structures from families A and B are shown in blue and purple, respectively. The backbone atoms (N, Cα, and *C*O) of residues 1−6 were used for the superimposition and the rmsd calculations.

and B, respectively. Thus, the backbone of family A has a better resemblance with desmopressin than family B, especially for the part of the backbone belonging to the γ-turn mimetic. In both structure families, the side chains of residues Tyr2 and Phe3 are positioned only slightly differently than in desmopressin. In contrast, the side chain of Asn5, which is critical for the antidiuretic activity,[48] points away from the macrocyclic ring in family B whereas it lies over the macrocycle both in desmopressin and in family A of **4**. The three residue tail is flexible both in **4** and in desmopressin, but because the same hydrogen bonds are observed in this region for both compounds, the conformation of the tail appears to be unaffected by the inverse γ-turn mimetic. Even though the covalently linked backbone of the inverse γ-turn mimetic makes **4** more rigid than desmopressin, structural family A mimics the structure of desmopressin fairly well. It therefore appears that conformational influences from the inverse γ-turn mimetic in **4** are, on their own, insufficient to explain the very low antidiuretic effect found for **4** (Table 1). Instead, it seems that the covalent modifications in the mimetic part of **4**, i.e., the methylene ether isostere or the methylene bridge, may be responsible for the loss of antidiuretic activity; this was a hypothesis that was probed further with desmopressin analogue **8**.

Analogue **8** has a very good conformational resemblance to desmopressin, as revealed by comparison of the lowest energy structures of **8** and desmopressin (Figure 6). In this case, the rmsd for the backbone atoms of residues 1−6 in the superimposition is only 0.66 Å. The methylene ether isostere in **8** does not allow formation of the hydrogen bond between Phe3 CO and Asn5 NH, which is found in the inverse γ-turn of desmopressin.[14] Despite this, the backbone conformation of an inverse γ-turn is well-conserved in **8**. In addition, the positions of the side chains of Tyr2, Phe3, and Asn5 deviate only slightly from those of desmopressin. The close similarity between the conformations adopted by **8** and desmopressin reveals that the low biological activity of **8** is most certainly due to the amide bond between Phe3 and Gln4 in desmopressin has a crucial

Figure 6. Comparison of the lowest energy strutures found in aqueous solution for desmopressin[14] and peptide **8**. Desmopressin is represented in green, and **8** is represented in red. The backbone atoms (N, Cα, and *C*O) of residues 1−6 were used for the superimposition and the rmsd calculations.

role in interactions with the antidiuretic V_2 receptor. We interpret our data as suggesting that this amide bond is involved in hydrogen bonding with the G-protein-coupled receptor. Lack of an amide bond between residues 3 and 4 also explains the loss of bioactivity displayed by analogues **4** and **6** (Table 1), which contain γ-turn mimetics instead of residues Phe3−Asn5. The fact that **4** and **6** are approximately 2 orders of magnitude less potent than **8** may be because

the γ-turn mimetic makes the rest of the macrocyclic ring in **4** and **6** more rigid and/or the methylene bridge provides additional hindrance for receptor binding. It is also possible that analogue **8**, just as desmopressin, is able to adopt γ- or β-turn conformations in the macrocyclic ring depending on the environment, thereby explaining the increased potency of **8** as compared to **4** and **6**.[49] Finally, the data presented in this paper suggest that desmopressin does not bind to the V_2 receptor with residues Phe3−Asn5 oriented as a γ-turn.

Conclusions. Two analogues of desmopressin (**4** and **6**), in which γ-turn mimetics were inserted instead of residues Phe3−Asn5, have been prepared to probe the interactions between desmopressin and the V_2 G-protein-coupled receptor. An analogue (**8**) having a methylene ether isostere in place of the amide bond between residues 3 and 4 was also synthesized to further aid the structure−activity studies. Conformational studies based on 2D NMR spectroscopy revealed that one of the two structural families found for analogue **4** (which contains a mimetic of an inverse γ-turn) mimicked the lowest energy conformation determined for desmopressin in aqueous solution fairly well. Moreover, the minimum energy conformation found for analogue **8** resembled that of desmopressin very well. Analogues **4** and **6** were both more than 5 orders of magnitude less active as antidiuretics than desmopressin when administered intravenously to rats, whereas analogue **8** was more active than **4** and **6** but still 3 orders of magnitude less active than desmopressin. The good conformational resemblance between the analogues and desmopressin, together with the low antidiuretic activity displayed by the analogues, revealed that the amide bond between Phe3 and Gln4 in desmopressin has a crucial role in interactions with the antidiuretic V_2 receptor. Most likely, this amide bond is involved in hydrogen bonding with the G-protein-coupled receptor. In addition, this investigation does not support the presence of an inverse γ-turn involving residues Phe3−Asn5 when desmopressin is bound to the V_2 receptor.

Experimental Section

General. The reactions in the synthesis of **7** were carried out under an inert atmosphere with dry solvents under anhydrous conditions. CH_2Cl_2 and 1,4-dioxane were dried by distillation from calcium hydride and sodium benzophenone, respectively. Dimethylformamide (DMF) was distilled before use in solid phase peptide synthesis. Thin-layer chromatography (TLC) was performed on Silica Gel 60 F_{254} (Merck) with detection by UV light and charring with phosphomolybdic acid in EtOH (26 mM). Flash column chromatography (eluents given in brackets) was performed on silica gel (Matrex, 60 Å, 35−70 mm, Grace Amicon).

The ^{1}H and ^{13}C NMR spectra of compounds **7** and **10** were recorded at 400 and 100 MHz, respectively, on a Bruker DRX-400 spectrometer for solutions in $CDCl_3$ [residual $CHCl_3$ (δ_H 7.26 ppm) or $CDCl_3$ (δ_C 77.0 ppm) as internal standard] at 298 K. IR spectra were recorded on an ATI Mattson Genesis Series FTIR spectrometer. Optical rotations were measured with a Perkin-Elmer 343 polarimeter. Positive fast atom bombardment mass spectra (FABMS) were recorded on a JEOL SX102 A mass spectrometer. Ions for FABMS were produced by a beam of Xenon atoms (6 keV) from a matrix of glycerol and thioglycerol. In the amino acid analysis, asparagine was determined as aspartic acid.

Peptide **4**[26] and compound **5**[26] were prepared as described in the cited reference. (2*S*)-2-Amino-3-phenylpropanol (**9**) was purchased from Aldrich (U.S.A.).

(2*S*)-2-Azido-3-phenylpropanol (10). First, triflic azide (TfN_3, caution[31]) was prepared by addition of freshly distilled triflic anhydride (1.35 mL, 8.01 mmol) to a mixture of NaN_3 (2.60 g, 40 mmol) in H_2O (6 mL) and CH_2Cl_2 (10 mL) at 0 °C. The mixture was stirred vigorously for 2 h at 0 °C, and the phases were separated. The water phase was extracted two times with a small amount of CH_2Cl_2, and the combined organic layers were washed with saturated aqueous $NaHCO_3$. Then, **9** (0.287 g, 1.90 mmol), 4-(dimethylamino)pyridine (0.126 g, 1.03 mmol), and $CuSO_4$ (18 mg) were dissolved in CH_2Cl_2 (2 mL). The TfN_3 solution (10 mL) was added dropwise, and while it was stirred for 2 h at room temperature, the color changed from blue to green. The solution was washed twice with 10% aqueous citric acid, twice with saturated aqueous $NaHCO_3$, and twice with brine. The organic layer was dried over $MgSO_4$, filtered, and concentrated. Flash column cromatography (heptane−EtOAc, 2:1) of the residue gave **10** (0.229 g, 68%) as a colorless oil; $[\alpha]_D^{20} = -1.9°$ (*c* 1.0, CH_2Cl_2). ^{1}H NMR: δ 7.38−7.25 (m, 5H, Ph), 3.72 (m, 2 H, CH_2O and CHN_3), 3.57 (m, 1 H, CH_2O), 2.89 (dd, J = 13.6 and 6.1 Hz, 1 H, PhCH_2), 2.84 (dd, J = 13.6 and 6.1 Hz, 1 H, PhCH_2), 2.62 (br. s, 1 H, OH). ^{13}C NMR: δ 137.2, 129.4 (2 C), 128.8 (2 C), 127.1, 65.4, 64.5, 37.1. IR (neat): n = 3345 (OH), 2108 (N_3). HR FABMS calcd for $C_9H_{11}N_3O$ (M + H), 178.0980; found, 178.0981.

(2*S*)-2-[(2*S*)-2-Azido-3-phenylpropyloxy]propionic Acid (7). (2*R*)-2-Chloropropionic acid (125 mg, 1.15 mmol) followed by NaH (50% in mineral oil, 610 mg, 12.7 mmol) was added to **10** (89 mg, 0.50 mmol) in dry 1,4-dioxane (25 mL) at room temperature. After it was stirred for 20 h, H_2O (8 mL) was added to destroy the excess of NaH. The resulting aqueous phase was washed with heptane and then acidified to pH 2−3 with aqueous HCl (2 M). The aqueous phase was extracted with CH_2Cl_2, and the organic phase was washed with water, dried over Na_2SO_4, filtered, and concentrated. Flash column chromatography (heptane−EtOAc−AcOH, 80:16:4) of the residue gave **7** (60 mg, 48%) as a colorless oil; $[\alpha]_D^{20} = -13.3°$ (*c* 1.0, CH_2Cl_2). ^{1}H NMR: δ = 10.11 (br. s, 1 H, COOH), 7.40−7.20 (m, 5 H, Ph), 4.05 (q, J = 6.9 Hz, 1 H, CHCH$_3$), 3.83 (m, 2 H, CH_2O and CHN_3), 3.41 (dd, J = 10.3 and 8.0 Hz, 1 H, CH_2O), 2.77 (dd, J = 13.5 and 8.0 Hz, 1 H, PhCH_2), 2.68 (dd, J = 13.5 and 5.8 Hz, 1 H, PhCH_2), 1.52 (d, J = 7.0 Hz, 3 H, CH_3). ^{13}C NMR: δ 178.7, 137.1, 129.3 (2 C), 128.7 (2 C), 127.0, 75.4, 72.5, 62.8, 37.2, 18.5. IR (neat): ν = 2121 (N_3), 1722 (C=O). HR FABMS calcd for $C_{12}H_{15}N_3O_3$ (M + H), 250.1192; found, 250.1192.

Solid Phase Synthesis of Peptides 6 and 8. Peptides **6** and **8** were synthesized on solid phase using the Fmoc strategy with DMF as solvent in a mechanically agitated reactor. ArgoGel−RINK (0.67 mmol/g, 388 mg, 260 mmol) was used as solid support for **6**, whereas TentaGel S NH_2 (0.27 mmol/g, 296 mg, 80 mmol) functionalized with the Rink linker[33,34] was used for **8**. N^{α}-Fmoc amino acids with side chain protecting groups were used as follows: 2,2,5,7,8-pentamethylchroman-6-sulfonyl (Pmc) for D-Arg; triphenylmethyl (Trt) for Asn, Cys, and 3-mercaptopropionic acid; and *tert*-butyl (*t*Bu) for Tyr.

The Rink linker, N^{α}-Fmoc amino acids, and mercaptopropionic acid were coupled to the resin after activation as HOBt esters.[35] These were prepared in situ by treatment of the appropiate acid (4 equiv) with 1-hydroxybenzotriazole (HOBt; 6 equiv) and 1,3-diisopropylcarbodiimide (DIC; 3.9 equiv) in freshly distilled DMF (1−1.5 mL) during 30−60 min. Building blocks **5** (40 mg, 65 mmol, 0.25 equiv) and **7** (32 mg, 130 mmol, 1.6 equiv) were activated with 1-hydroxy-7-azabenzotriazole[36] (HOAt; 0.38 equiv for **5**, 2.5 equiv for **7**) and DIC (0.3 equiv for **5**, 1.5 equiv for **7**) in DMF (1 mL). Couplings were performed during 1−2 h and monitored by using bromophenol blue[50] (0.05% of the resin capacity) as indicator of unacylated amino groups on the peptide resin. N^{α}-Fmoc deprotection was achieved by a slow flow of 20% piperidine in DMF through the reactor (4 min), followed by addition of the piperidine solution to the reactor and rotation during 7 min. After each deprotection, the resin was washed with DMF. After incorporation of building block **5**, which was coupled to an excess of

resin, the remaining nonacylated amino groups on the peptide resin were capped by treatment with acetic anhydride. The resin was then washed with CH_2Cl_2 (5 × 2 mL) and dried in vacuo. Incorporation of **5** and **7** was confirmed by IR spectroscopy on a few resin beads,[37] which showed an N_3 stretch at 2119 cm^{-1}. Reduction of the azido group[29] was achieved by sequential addition of triethylamine (280 mL, 2 mmol), thiophenol (165 mL, 1.6 mmol), and anhydrous $SnCl_2$ (75.8 mg, 0.4 mmol) to the resin suspended in tetrahydrofuran (THF; 1 mL). After 20 h, the resin was washed with THF (8 × 2 mL), 20% piperidine in DMF (2 mL, 5 min), and CH_2Cl_2 (8 × 2 mL) and dried in vacuo. The disappearance of the N_3 stretch in the IR spectrum indicated a successful reduction. The resin was then suspended in DMF (1 mL), and the synthesis was continued as described above.

After completion of the synthesis, the resin was washed with CH_2Cl_2 (8 × 2 mL) and dried in vacuo. Each of the peptides were cleaved from a portion of the resins, and the amino acid side chains were deprotected, by treatment with trifluoroacetic acid/water/thioanisole/ethanedithiol (87.5:5:5:2.5) for 2 h followed by filtration. Acetic acid was added to the filtrate, the solution was concentrated, and acetic acid (3 × 5 mL) was added again followed by concentration after each addition. The residue was triturated with diethyl ether. The diethyl ether solution was decanted, and the solid, crude peptide was dissolved in acetic acid/water (1:5) and freeze-dried. At this stage, the precursor of peptide **6** was purified with reversed-phase HPLC prior to oxidation in order to remove the capped tetrapeptide. Cyclization[25] was performed by alternating additions of portions of the crude peptide in acetic acid and I_2 in methanol (0.1 M) to 10% acetic acid in methanol (2 mL/mg cleaved resin). After the final addition of I_2, a light brown solution was obtained, which was neutralized and decolorized by stirring with Dowex 2 × 8 anion exchange resin (Fluka, 50−100 mesh, converted from Cl^- to acetate form by washing with 1 M aqueous NaOH, water, acetic acid, water, and methanol), filtrated, and concentrated. The peptide was then dissolved in water and freeze-dried.

Peptides **6** and **8** were purified on a Beckman System Gold HPLC using a Kromasil C-8 column (100 Å, 5 μm, 20 mm × 250 mm) and a gradient of 0−80% of B in A over 60 min (solvent systems: A, 0.1% aqueous trifluoroacetic acid, and B, 0.1% trifluoroacetic acid in acetonitrile, flow rate: 11 mL/min) with detection at 214 nm. This gave peptides **6** (11.3 mg, 17% based on the amount of **5** employed) and **8** (11 mg, 23% based on the amount of resin employed).

Peptide **6** had FABMS calcd for $C_{45}H_{63}N_{12}O_{11}S_2$ 1011 (M + H); found, 1011. Amino acid analysis: Arg 0.99 (1), Cys 1.00 (1), Gly 1.02 (1), Pro 1.00 (1), Tyr 0.98 (1). ^{1}H NMR data are given in Table 3.

Peptide **8** had FABMS calcd for $C_{44}H_{63}N_{12}O_{11}S_2$ 999 (M + H); found, 999. Amino acid analysis: Arg 0.99 (1), Asp 1.02 (1), Cys 0.96 (1), Gly 1.02 (1), Pro 1.02 (1), Tyr 0.98 (1). ^{1}H NMR data are given in Table 5.

Agonistic and Antagonistic Properties of Peptides 4, 6, and 8 at the Vasopressin Receptor. Vasopressin (**1**) was used as control and agonist (561.3 IU/mg) and stock solutions of **1**, **4**, **6**, and **8** were made in 0.9% NaCl. Female Sprague−Dawley rats (184−221 g) were anaesthetized i.p. with Inactin in the afternoon before each study. A tracheostomy was performed, and catheters were introduced in the jugular vein and in the urethra. Hydration with a hypoosmotic solution was started immediately after surgery had been completed. In the morning of the study, the urethral catheters were connected to a conductometer connected to an amplifier and a computer for registration of urine conductivity, which was used as readout for the antidiuretic response. The compound investigated was administered in 0.9% NaCl (0.2 mL) through the catheter in the jugular vein. Each experiment was started by giving the animal a "reactivity dose" of **1**.

The agonistic, i.e., the antidiuretic, activity was then determined as described previously.[51] Each animal received two doses of **1** and two doses of the peptide under investigation to give a 2 × 2 assay, and each peptide was investigated at two different occasions. When the peptide under investigation had a low activity, only one dose of the peptide was given. One injection of saline was also given to each animal.

The antagonistic activity was determined by giving each animal three doses of **1** thereby creating a dose−response curve. A dose of the peptide under investigation was given 10 min prior to a dose of **1**, chosen in the linear part of the dose−response curve.

Preparation of NMR Samples. Desmopressin analogue **4** (4.4 mg) was dissolved in phosphate buffer (20 mM, pH 6.7, 550 mL), which contained 10% D_2O to give an ∼8 mM solution. Another aqueous sample of **4**, having a concentration of ∼20 mM, was preperad in the same manner and used for the NOESY experiment. No aggregation of **4** was detected at these concentrations. Analogue **6** was dissolved in the same buffer as **4** to give an ∼10 mM sample. Analogue **8** (5 mg) was dissolved in phosphate buffer (40 mM, pH 6.6, 550 mL), which contained 10% D_2O to give an ∼9 mM solution. The phosphate buffers contained 0.3 mM NaN_3 (0.3 mM) to prevent bacterial growth. In all samples, the pH was adjusted to the original value of the buffer by addition of small aliquots of solutions of aqueous 0.1 M NaOH or HCl.

NMR Experiments. DQF−COSY,[52] TOCSY,[53] NOESY,[54] ROESY,[55] and gradient-enhanced ^{1}H−^{13}C-HSQC[56] experiments were recorded on a 600 MHz Bruker DRX instrument at 5 °C for peptides, **4**, **6**, and **8**. Temperature gradient experiments were conducted with a 500 MHz Bruker AMX spectrometer. The water resonance at 4.98 ppm was used as an internal shift reference. NOESY spectra for **4** and **6** were recorded with a mixing time of 200 ms. The ROESY spectrum for **8** was recorded with a spin-lock field strength of ∼4.5 kHz and a mixing time of 150 ms. A DIPSI-2 mixing sequence[57] was used in the TOCSY experiments with a spin-lock time of 86 ms. COSY, TOCSY, and ^{1}H−^{13}C-HSQC experiments were recorded with 2048 complex data points in t_2 and 512 increments in t_1. Linear prediction in t_1 resulted in a final data matrix of 2 K × 1 K complex data points. NOESY and ROESY spectra were recorded with 2048 complex data points in t_2 and 800 increments in t_1. Zero-filling and linear prediction up to 1 K resulted in a final data matrix of 4 K × 2 K. Apodization with a shifted square sine bell function was performed in both dimensions prior to Fourier transformation in all experiments except COSY where a sine bell function was used. WATERGATE[58] was used for water suppression in the ROESY, NOESY, and TOCSY experiments. Amide proton temperature coefficients were determined from a series of ^{1}H NMR spectra acquired at temperatures ranging from 5 to 40 °C with presaturation during the relaxation delay. The amide proton shifts were adjusted with regard to the temperature dependence of the water signal (−11.9 ppb/K).[59] All processing was performed in XWINNMR (Bruker) on a SGI O_2 workstation.

Assignment and Structure Determination. Proton resonance assignment for peptides **4**, **6**, and **8** was obtained using the conventional strategy.[38] Initial spin system recognition was obtained from the COSY and TOCSY spectra. Sequential assignment could subsequently be made with use of the NOESY or ROESY spectra. The complete proton resonance assignment was used together with the gradient-enhanced ^{1}H−^{13}C-HSQC spectra to assign the ^{13}C resonances.

Peak volumes from assigned cross-peaks in the NOESY (for **4**) and ROESY (for **8**) spectra were converted to interproton distances, d_{ij}, by using the isolated spin pair approximization

$$d_{ij} = d_{\mathrm{ref}}(V_{\mathrm{ref}}/V_{ij})^{1/6}$$

in which d_{ref} corresponds to a known interproton distance. V_{ref} and V_{ij} are the volumes of the reference cross-peak and peak ij, respectively. The mean value of the cross-peak volumes from the geminal β-methylene protons in Phe3 and Cys6 was used as V_{ref} for **4**. Because of overlap, only the cross-peak from the β-methylene protons in Phe3 could be used to determine V_{ref} for **8**. The reference distance d_{ref} was set to 1.77 Å for both **4** and **8**. In the structure calculations, the lower distance limit for d_{ij} was set to 1.80 Å and the upper distance limit was set

to 10% above the determined distance. Methyl, methylene, and aromatic ring protons with degenerate shifts were treated as pseudoatoms. Upper distance limits for distance restraints involving these pseudoatoms were increased by 1.0, 0.9, and 1.2 Å, respectively.[60]

NOESY peak picking and cross-peak volume integration for **4** were performed in XWINNMR. $J_{NH\alpha}$ was measured from the line widths in the NOESY spectrum according to the method of Wang et al.[61] $J_{\alpha\beta}$ was determined by simulating the observed COSY cross-peaks with the programs SPHINX and LINSHA.[62] Coupling constants were converted into dihedral angles using the Karplus equation. Those values for $^3J_{\alpha\beta}$ that were compatible with the NOEs were chosen as dihedral angle restraints for the structure calculations. Peak picking and ROESY cross-peak integrations for **8** were performed in FELIX,[63] which was also used to extract $^3J_{HN\alpha}$. Because of spectral overlap, no $^3J_{\alpha\beta}$ was estimated.

Three-dimensional starting structures were determined from NMR data with the program X-PLOR.[41] Structures generated within X-PLOR were subjected to simulated annealing using an ab initio simulated annealing protocol followed by simulated annealing refinement.[42,43] Two starting structures with different conformations were used to sample more of the conformational space. The initial temperature in the annealing protocol was set to 1000 K, and the final temperature was 100 K. All structures were minimized with a 200 step Powell minimization after refinment. A soft square-welled potential with a force constant of 50 kcal mol^{-1} $Å^{-2}$ was used for the NOE distance restraints, and a square well potential with a force constant of 1 kcal mol^{-1} rad^{-2} was used for the dihedral angle restraints. In all calculations, only structures with no distance restraint violations larger than 0.3 Å and no dihedral angle restraint violations larger than 5° were accepted. All structure calculations were performed on SGI O_2 workstations. Root mean square deviation values and superimpositions were obtained using the backbone and heavy atoms of residues 1−6. The average structures of both peptides were calculated in X-PLOR from the accepted structures and were then used as comparison coordinate sets for the rmsd calculations.

Acknowledgment. This work was funded by grants from the Swedish Research Council, the Biotechnology Fund at Umeå University, and the Göran Gustafsson Foundation for Research in Natural Sciences and Medicine.

References

(1) du Vigneaud, V.; Lawler, H. C.; Popenoe, E. A. Enzymatic cleavage of glycinamide from vasopressin and a proposed structure for this pressor-antidiuretic hormone of the posterior pituitary. *J. Am. Chem. Soc.* **1953**, *75*, 4880−4881.

(2) Michell, R. H.; Kirk, C. J.; Billah, M. M. Hormonal stimulation of phosphatidylinositol breakdown, with particular reference to the hepatic effects of vasopressin. *Biochem. Soc. Trans.* **1979**, *7*, 861−865.

(3) Vávra, I.; Machová, A.; Holecek, V.; Cort, J. H.; Zaoral, M.; Sorm, F. Effect of a synthetic analogue of vasopressin in animals and in patients with diabetes insipidus. *Lancet* **1968**, 948−952.

(4) Zaoral, M. Vasopressin analogues with high and specific antidiuretic activity. *Int. J. Pept. Protein Res.* **1985**, *25*, 561−574.

(5) Mannucci, P. M.; Åberg, M.; Nilsson, I. M.; Robertsson, B. Mechanism of plasminogen activator and factor VIII increase after vasoactive drugs. *Br. J. Haematol.* **1975**, *30*, 81−93.

(6) Cash, J. D.; Gader, A. M. A.; Da Costa, J. The release of plasminogen activator and factor VIII to lysine vasopressin, arginine vasopressin, 1-desamino-8-D-arginine vasopressin, angiotensin and oxytocin in man. *Br. J. Haematol.* **1974**, *27*, 363−364.

(7) Plattner, J. J.; Norbeck, D. W. Obstacles to drug development from peptide leads. In *Drug Discovery Technologies*; Clark, C. R., Moos, W. R., Eds.; Ellis Harwood Ltd.-Halstead Press: Chichester, England, 1989; pp 92−126.

(8) Ball, J. B.; Alewood, P. F. Conformational constraints: Nonpeptide β-turn mimics. *J. Mol. Recognit.* **1990**, *3*, 55−64.

(9) Hölzemann, G. Peptide conformation mimetics. *Kontakte (Darmstadt)* **1991**, 3−12, 55−63.

(10) Kahn, M. Peptide Secondary Structure Mimetics: Recent Advances and Future Challenges. *Synlett* **1993**, 821−826.

(11) Giannis, A.; Kolter, T. Peptidomimetics for receptor ligands-discovery, development, and medical perspectives. *Angew. Chem., Int. Ed. Engl.* **1993**, *32*, 1244−1267.

(12) Liskamp, R. M. J. Conformationally restricted amino acids and dipeptides, (non)peptidomometics and secondary structure mimetics. *Recl. Trav. Chim. Pays-Bas* **1994**, *113*, 1−19.

(13) Wang, J.; Hodges, R. S.; Sykes, B. D. Generating multiple conformations of flexible peptides in solution based on NMR nuclear overhauser effect data: Application to desmopressin. *J. Am. Chem. Soc.* **1995**, *117*, 8627−8634.

(14) Walse, B.; Kihlberg, J.; Drakenberg, T. Conformation of desmopressin, an analogue of the peptide hormone vasopressin, in aqueous solution as determined by NMR spectroscopy. *Eur. J. Biochem.* **1998**, *252*, 428−440.

(15) Wang, J.; Breslow, E.; Sykes, B. D. Differential binding of desmopressin and vasopressin to neurophysin-II. *J. Biol. Chem.* **1996**, *271*, 31354−31359.

(16) Hruby, V. J.; Lebl, M. I. Conformational properties of neurohypophyseal hormone analogues in solution as determined by NMR and laser Raman spectroscopies. In *CRC Handbook of Neurohypophyseal Hormone Analogues*; Jost, K., Lebl, M., Brtnik, F., Eds.; CRC Press: Boca Raton, FL, 1987; pp 105−155.

(17) Schmidt, J. M.; Ohlenschläger, O.; Rüterjans, H.; Grzonka, Z.; Kojro, E.; Pavo, I.; Fahrenholz, F. Conformation of [8-arginine]-vasopressin and V_1 antagonists in dimethyl sulfoxide solution derived from two-dimensional NMR spectroscopy and molecular dynamics simulation. *Eur. J. Biochem.* **1991**, *201*, 355−371.

(18) Shenderovich, M. D.; Kasprzykowski, F.; Liwo, A.; Sekacis, I.; Saulitis, J.; Nikiforovich, G. V. Conformational analysis of [Cpp1, Sar7, Arg8]vasopressin by ^{1}H NMR spectroscopy and molecular mechanics calculations. *Int. J. Pept. Protein Res.* **1991**, *38*, 528−538.

(19) Zieger, G.; Andreae, F.; Sterk, H. Assignment of proton NMR resonances and conformational analysis of [Lys8]-vasopressin homologues. *Magn. Reson. Chem.* **1991**, *29*, 580−586.

(20) Yu, C.; Yang, T.-H.; Yeh, C.-J.; Chuang, L.-C. Combined use of NMR, distance geometry, and restrained energy minimization for the conformational analysis of 8-lysine-vasopressin. *Can. J. Chem.* **1992**, *70*, 1950−1955.

(21) Nutz, K. I.; Fabian, W. M. F.; Sterk, H. Conformations of triglycyllysylvasopressin: ^{1}H NMR spectroscopic and molecular dynamics study. *Magn. Reson. Chem.* **1993**, *31*, 481−488.

(22) Mouillac, B.; Chini, B.; Balestre, M.-N.; Elands, J.; Trumpp-Kallmeyer, S.; Hoflack, J.; Hibert, M.; Jard, S.; Barberis, C. The binding site of neuropeptide vasopressin V1a receptor, evidence for a major localization within transmembrane regions. *J. Biol. Chem.* **1995**, *270*, 25771−25777.

(23) Cort, J. H.; Fric, I.; Carlsson, L.; Gillessen, D.; Bystricky, S.; Skopkova, J.; Gut, V.; Studer, R. O.; Mulder, J. L.; Blaha, K. Biological and chiroptical sequelae of graded alkyl substitutions in the vasopressin ring. *Mol. Pharmacol.* **1976**, *12*, 313−321.

(24) Johansson, B.; Ferring, A.B. Unpublished results.

(25) Kihlberg, J.; Åhman, J.; Walse, B.; Drakenberg, T.; Nilsson, A.; Söderberg-Ahlm, C.; Bengtsson, B.; Olsson, H. Glycosylated peptide hormones: Pharmacological properties and conformational studies of analogues of [1-Desamino,8-D-arginine]vasopressin. *J. Med. Chem.* **1995**, *38*, 161−169.

(26) Brickmann, K.; Yuan, Z.; Sethson, I.; Somfai, P.; Kihlberg, J. Synthesis of conformationally restricted mimetics of γ-turns and incorporation in desmopressin, an analogue of the peptide hormone vasopressin. *Chem. Eur. J.* **1999**, *5*, 2241−2253.

(27) Barth, T.; Velek, J.; Barthova, J.; Velkova, V.; Jezek, J.; Hauzerova, L.; Kasicka, V.; Ubik, K.; Machova, A.; Vilhardt, H. Metabolism of Desmopressin ([8-D-Arginine]deaminovasopressin) by the enzymes of gastrointestinal tract. In *Peptides 1998: Proceedings of the Twenty-Fifth European Peptide Symposium*; Bajussz, S., Hudecz, F., Eds.; Akadémiai Kiado: Budapest, Hungary, 1999; pp 862−863.

(28) Emtenäs, H. An approach to a peptide mimetic for incorporation into DDAVP. Masters Thesis, Umeå University, Umeå, 1998.

(29) Bartra, M.; Romea, P.; Urpi, F.; Vilarrasa, J. A fast procedure for the reduction of azides and nitro compounds based on the reducing ability of $Sn(SR)_3$- species. *Tetrahedron* **1990**, *46*, 587−594.

(30) Alper, P. B.; Hung, S.-C.; Wong, C.-H. Metal catalyzed diazo transfer for the synthesis of azides from amines. *Tetrahedron Lett.* **1996**, *37*, 6029−6032.

(31) Triflic azide has been reported to be explosive if dry and should always be used as a solution (cf. Caveander, C. J.; Shiner, V. J. *J. Org. Chem.* **1972**, *37*, 3567−3569).

(32) Andersson, L.; Kenne, L. Synthesis and NMR studies of methyl 3-*O*-[(*R*)- and (*S*)-1-carboxyethyl]-α−D-gluco-, galacto- and mannopyranosides. *Carbohydr. Res.* **1998**, *313*, 157−164.

(33) Rink, H. Solid-phase synthesis of protected peptide fragments using a trialkoxy-diphenyl-methylester resin. *Tetrahedron Lett.* **1987**, *28*, 3787−3790.

(34) Bernatowicz, M. S.; Daniels, S. B.; Köster, H. A comparison of acid labile linkage agents for the synthesis of peptide *C*-terminal amides. *Tetrahedron Lett.* **1989**, *30*, 4645−4648.
(35) König, W.; Geiger, R. A new method for synthesis of peptides: Activation of the carboxyl group with dicyclohexylcarbodiimide using 1-hydroxybenzotriazoles as additives. *Chem. Ber.* **1970**, *103*, 788−798.
(36) Carpino, L. A. 1-Hydroxy-7-azabenzotriazole. An efficient peptide coupling additive. *J. Am. Chem. Soc.* **1993**, *115*, 4397−4398.
(37) Kick, E. K.; Ellman, J. A. Expedient method for the solid-phase synthesis of aspartic acid protease inhibitors directed toward the generation of libraries. *J. Med. Chem.* **1995**, *38*, 1427−1430.
(38) Wüthrich, K. *NMR of Proteins and Nucleic Acids*; John Wiley & Sons Inc.: New York, 1986.
(39) Spectra were recorded at 5 °C to reduce the tumbling rate of **4** and thereby enhance the quality of the NOESY spectrum. In addition, this allows comparison with the structure determined previously for desmopressin at 5 °C.
(40) Kline, A. D.; Braun, W.; Wüthrich, K. Determination of the complete three-dimenisonal structure of the α-amylase inhibitor tendamistat in aqueous solution by nuclear magnetic resonance and distance geometry. *J. Mol. Biol.* **1988**, *204*, 675−694.
(41) Brünger, A. T. *X-PLOR, Version 3.1. A System for X-ray Crystallography and NMR*; Yale Universtity Press: New Haven, CT, 1992.
(42) Nilges, M.; Clore, G. M.; Gronenborn, A. M. Determination of three-dimensional structures of proteins from interproton distance data by dynamical simulated annealing from a random array of atoms. *FEBS Lett.* **1988**, *239*, 129−136.
(43) Nilges, M.; Kuszewski, J.; Brunger, A. T. *Computational Aspects of the Study of Biological Macromolecules by NMR*; Plenum Press: New York, 1991.
(44) Kessler, H.; Griesinger, C.; Lautz, J.; Müller, A.; van Gunsteren, W. F.; Berendsen, H. J. C. Conformational dynamics detected by nuclear magnetic resonance NOE values and *J* coupling constants. *J. Am. Chem. Soc.* **1988**, *110*, 3393−3396.
(45) Frisch, M. J.; Trucks, G. W.; Schlegel, H. B.; Scuseria, G. E.; Robb, M. A.; Cheeseman, J. R.; Zakrzewski, V. G.; Montgomery, J. A., Jr.; Stratmann, R. E.; Burant, J. C.; Dapprich, S.; Millam, J. M.; Daniels, A. D.; Kudin, K. N.; Strain, M. C.; Farkas, O.; Tomasi, J.; Barone, V.; Cossi, M.; Cammi, R.; Mennucci, B.; Pomelli, C.; Adamo, C.; Clifford, S.; Ochterski, J.; Petersson, G. A.; Ayala, P. Y.; Cui, Q.; Morokuma, K.; Malick, D. K.; Rabuck, A. D.; Raghavachari, K.; Foresman, J. B.; Cioslowski, J.; Ortiz, J. V.; Stefanov, B. B.; Liu, G.; Liashenko, A.; Piskorz, P.; Komaromi, I.; Gomperts, R.; Martin, R. L.; Fox, D. J.; Keith, T.; Al-Laham, M. A.; Peng, C. Y.; Nanayakkara, A.; Gonzalez, C.; Challacombe, M.; Gill, P. M. W.; Johnson, B. G.; Chen, W.; Wong, M. W.; Andres, J. L.; Head-Gordon, M.; Replogle, E. S.; Pople, J. A. *Gaussian 98*, revision 5.2; Gaussian, Inc.: Pittsburgh, PA, 1998.
(46) The calculated hydrogen bond is a result of the NOE restrictions, but it is not reflected by the value of the temperature coefficient of D-Arg8 NH (cf. Table 2). Consequently, the structure calculations may give a less accurate description of the flexible, three residue tail of **4**.
(47) Wang, J.; Hodges, R. S.; Sykes, B. D. Effect of trifluoroethanol on the solution structure and flexibility of desmopressin: a two-dimensional NMR study. *Int. J. Pept. Protein Res.* **1995**, *45*, 471−481.
(48) Hruby, V. J.; Smith, C. W. Structure−Activity Relationships of Vasopressin Agonists. In *Chemistry, Biology, and Medicine of Neurohypophyseal Hormones and Their Analogues*; Smith, C. W., Ed.; Academic Press: Orlando, FL, 1987; pp 179−188.
(49) NMR spectra recorded for analogue **8** in 20% aqueous trifluoroethanol revealed minor changes in chemical shifts and NOEs as compared to spectra recorded in aqueous solution, thus providing some support for this hypothesis.
(50) Flegel, M.; Sheppard, R. C. A sensitive general method for quantitative monitoring of continuous flow solid-phase peptide synthesis. *J. Chem. Soc., Chem. Commun.* **1990**, 536−538.
(51) Larsson, L.-E.; Lindeberg, G.; Melin, P.; Pliska, V. Synthesis of O-alkylated lysine vasopressins. inhibitors of the antidiuretic response to lysine-vasopressin. *J. Med. Chem.* **1978**, *21*, 352−356.
(52) Aue, W. P.; Bartholdi, E.; Ernst, R. R. Two-dimensional spectroscopy. Application to nuclear magnetic resonance. *J. Chem. Phys.* **1976**, *64*, 2229−2246.
(53) Braunschweiler, L.; Ernst, R. R. Coherence transfer by isotropic mixing: Application to proton correlation spectroscopy. *J. Magn. Reson.* **1983**, *53*, 521−528.
(54) Macura, S.; Ernst, R. R. Elucidation of cross relaxation in liquids by two-dimensional N.M.R. spectroscopy. *Mol. Phys.* **1980**, *41*, 95−117.
(55) Bax, A.; Davis, D. G. Practical aspects of two-dimensional transverse NOE spectroscopy. *J. Magn. Reson.* **1985**, *63*, 207−213.
(56) Kay, L. E.; Keifer, P.; Saarinen, T. Pure absorption gradient enhanced heteronuclear single quantum correlation spectroscopy with improved sensitivty. *J. Am. Chem. Soc.* **1992**, *114*, 10663−10665.
(57) Shaka, A. J.; Lee, C. J.; Pines, A. Iterative schemes for bilinear operators; Application to spin decoupling. *J. Magn. Reson.* **1988**, *77*, 274−293.
(58) Piotto, M.; Saudek, V.; Sklenár, V. Gradient-tailored excitation for single-quantum NMR spectroscopy of aqueous solutions. *J. Biomol. NMR* **1992**, 661−665.
(59) Wishart, D. S.; Bigam, C. G.; Yao, J.; Abildgaard, F.; Dyson, H. J.; Oldfield, E.; Markley, J. L.; Sykes, B. D. ^{1}H, ^{13}C and ^{15}N chemical shift referencing in biomolecular NMR. *J. Biomol. NMR* **1995**, *6*, 135−140.
(60) Wüthrich, K.; Billeter, M.; Braun, W. Pseudo-structures for the 20 common amino acids for use in studies of protein conformations by measurements of intramolecular proton−proton distance constraints with nuclear magnetic resonance. *J. Mol. Biol.* **1983**, *169*, 949−961.
(61) Wang, Y.; Nip, A. M.; Wishart, D. S. A simple method to quantitatively measure polypeptide $J_{HNH\alpha}$ coupling constants from TOCSY or NOESY spectra. *J. Biomol. NMR* **1997**, *10*, 373−382.
(62) Widmer, H.; Wüthrich, K. Simulated two-dimensional NMR cross-peak fine structure for ^{1}H spin systems in polypeptides and polydeoxynucleotides. *J. Magn. Reson.* **1987**, *74*, 316−336.
(63) Accelrys Inc., www.accelrys.com.

JM011073B